REPORT DOCUMENTATION PAGE

1. REPORT DATE (DD-MM-YYYY)	2. REPORT TYPE	3. DATES COVERED (From - To)
December 2013	Technical Paper	December 2013- August 2014

4. TITLE AND SUBTITLE

Ab initio Kinetics of Methylamine Radical Thermal Decomposition and H-abstraction From Monomethylhydrazine by H Atom

5a. CONTRACT NUMBER
FA9300-06-C-0023

5b. GRANT NUMBER

5c. PROGRAM ELEMENT NUMBER

6. AUTHOR(S)

H. Sun, G. L. Vaghjiani, C. K. Law,

5d. PROJECT NUMBER

5e. TASK NUMBER

5f. WORK UNIT NUMBER
QORA

7. PERFORMING ORGANIZATION NAME(S) AND ADDRESS(ES)

Air Force Research Laboratory (AFMC)
AFRL/RQRP
10 E. Saturn Blvd.
Edwards AFB, CA, 93524-7680

8. PERFORMING ORGANIZATION REPORT NO.

9. SPONSORING / MONITORING AGENCY NAME(S) AND ADDRESS(ES)

Air Force Research Laboratory (AFMC)
AFRL/RQR
5 Pollux Drive.
Edwards AFB, CA, 93524-7048

10. SPONSOR/MONITOR'S ACRONYM(S)

11. SPONSOR/MONITOR'S REPORT NUMBER(S)

AFRL-RQ-ED-TP-2013-277

12. DISTRIBUTION / AVAILABILITY STATEMENT

Approved for public release; distribution unlimited

13. SUPPLEMENTARY NOTES

Technical Paper presented at 35th Int. Sym. on Combustion; San Francisco, CA, 3-8 Aug, 2014. PA# 14004

14. ABSTRACT

Methylamine radicals (CH3NH) and amino radicals (NH2) are the major products in the early ignition/pyrolysis of monomethylhydrazine (CH3NHNH2). The kinetics of thermal decomposition of CH3NH radicals was analyzed by RRKM master equation analysis. It was found that β scission of the methyl H atom from CH3NH radicals is dominant and fast enough to induce subsequent H-abstraction reactions to trigger ignition. The gas-phase kinetics of H-abstraction reactions from CH3NHNH2 by H atoms was further investigated by *ab initio* second-order multireference perturbation theory and quadratic-configuration-interaction calculations. It was found that the energy barriers for abstraction of the central amine H atom, two terminal amine H atoms, and methyl H atoms are: 2.95, 4.16, 5.98, and 8.50 kcal mol-1, respectively. In units of cm3 molecule-1 s-1, the corresponding rate coefficients were found to be: $k7 = 9.63\times10$-20T2.596exp($-154.2/T$); $k8 = 2.04\times10$-18T2.154 exp(104.1/T); $k9 = 1.13 \times 10$-20 T2.866 exp($-416.3/T$); $k10 = 2.41\times10$-23 T3.650 exp($-870.5/T$), respectively. The results reveal that abstraction of the terminal amine H atom to form trans-CH3NHN•H radicals is the dominant channel among the different abstraction channels. At 298K, the total theoretical H-abstraction rate coefficient, calculated with no adjustable parameters, is 8.16×10-13 cm3 molecule-1 s-1, which is in excellent agreement with the experimental observation of (7.60 ± 1.14)×10-13 cm3 molecule-1 s-1 (Vaghjiani, *J. Phys. Chem. A*, 1997).

15. SUBJECT TERMS

16. SECURITY CLASSIFICATION OF:			17. LIMITATION OF ABSTRACT	18. NUMBER OF PAGES	19a. NAME OF RESPONSIBLE PERSON
a. REPORT	**b. ABSTRACT**	**c. THIS PAGE**	SAR	19	G. Vaghjiani
Unclassified	Unclassified	Unclassified			**19b. TELEPHONE NO** (include area code) 661-275-5657

Ab initio Kinetics of Methylamine Radical Thermal Decomposition and H-abstraction from Monomethylhydrazine by H Atom

Hongyan Sun[1], Ghanshyam L. Vaghjiani[1], and Chung K. Law[2]
[1]Air Force Research Laboratory, AFRL/RQRP, Edwards AFB, California 93524, USA
[2]Department of Mechanical and Aerospace Engineering, Princeton University, Princeton, New Jersey 08544

Abstract

Methylamine radicals (CH_3NH) and amino radicals (NH_2) are the major products in the early ignition/pyrolysis of monomethylhydrazine (CH_3NHNH_2). The kinetics of thermal decomposition of CH_3NH radicals was analyzed by RRKM master equation analysis. It was found that β scission of the methyl H atom from CH_3NH radicals is dominant and fast enough to induce subsequent H-abstraction reactions to trigger ignition. The gas-phase kinetics of H-abstraction reactions from CH_3NHNH_2 by H atoms was further investigated by *ab initio* second-order multireference perturbation theory and quadratic-configuration-interaction calculations. It was found that the energy barriers for abstraction of the central amine H atom, two terminal amine H atoms, and methyl H atoms are: 2.95, 4.16, 5.98, and 8.50 kcal mol^{-1}, respectively. In units of cm^3 molecule^{-1} s^{-1}, the corresponding rate coefficients were found to be: $k_7 = 9.63 \times 10^{-20} T^{2.596} \exp(-154.2/T)$; $k_8 = 2.04 \times 10^{-18} T^{2.154} \exp(104.1/T)$; $k_9 = 1.13 \times 10^{-20} T^{2.866} \exp(-416.3/T)$; $k_{10} = 2.41 \times 10^{-23} T^{3.650} \exp(-870.5/T)$, respectively. The results reveal that abstraction of the terminal amine H atom to form trans-$CH_3NHN \bullet H$ radicals is the dominant channel among the different abstraction channels. At 298K, the total theoretical H-abstraction rate coefficient, calculated with no adjustable parameters, is 8.16×10^{-13} cm^3 molecule^{-1} s^{-1}, which is in excellent agreement with the experimental observation of $(7.60 \pm 1.14) \times 10^{-13}$ cm^3 molecule^{-1} s^{-1} (Vaghjiani, *J. Phys. Chem. A,* 1997).

Key words: CH_3NH decomposition, CH_3NHNH_2, H-abstraction, CASPT2, rate coefficient

1. Introduction

The binary system of monomethylhydrazine (CH_3NHNH_2) and dinitrogen tertroxide (N_2O_4) is widely used as liquid propellants for satellite and space propulsion applications [1]. It is known that the N—N bond strength is weaker than that of the C—N bond in CH_3NHNH_2, and as such, the CH_3NH and NH_2 radicals from N—N bond fission are the major products in the early ignition/pyrolysis of CH_3NHNH_2 [2]. Using the high-pressure limit rate coefficients of CH_3NHNH_2 decomposition [3], the branching ratio between the N—N bond fission and C—N bond fission was found to be 95:5 at a temperature of 1000K and for pressures in the range of 2 to 3 atm. To experimentally quantify the pressure-dependent rate coefficients for the N—N bond fission, Hanson's group [4] recently measured the NH_2 concentration time-histories in CH_3NHNH_2/Ar mixtures over the temperature range of 1100 to 1400K and pressures in the range of 0.3 to 5 atm behind reflected shock waves using laser absorption measurement methods. The fate of the CH_3NH radicals however was not reported. Theoretically, we have found that the CH_3NH radical is very reactive since direct β-scission of the methyl H atom in CH_3NH has a small energy barrier to form amino-methylene ($CH_2=NH$) as the stable product. Furthermore, the H atoms generated from this decomposition reaction will react with the unburned fuel molecules to induce ignition.

In this work, the kinetics of the thermal decomposition of CH_3NH radicals was analyzed and pressure dependent rate coefficients for the dominant reaction pathways determined by RRKM master equation analysis. Furthermore, the kinetics of H-abstraction from CH_3NHNH_2 by H atoms was analyzed using second-order multireference perturbation theory and unrestricted quadratic-configuration-interaction QCISD(T) calculations. The rate coefficients for each of the abstraction channels were quantified by micro-canonical transition state theory, and the associated branching ratios determined. It was found that the total rate coefficient determined from *ab initio* kinetics theories is in

excellent agreement with the experimental value observed at room temperature [5]. Thus the theoretical rate coefficients from this work should be reliable over a wide temperature range and are essential parameters in the development of reaction mechanisms for the kinetics modeling of ignition involving monomethylhydrazine and its derivatives.

2. Electronic Structures

There are several reaction pathways for the CH_3NH radical decomposition, which include β scission, isomerization, molecular elimination, and bond fission. The geometries of the stationary points of the potential energy surfaces (PESs) for these reactions were optimized at the B3LYP/6-311++G(d,p) level, except for bond fission reactions. For the C—N and N—H bond fission reactions in CH_3NH, multi-reference character of the wave functions is significant. Hence geometries of the transition states for these two bond breaking channels were optimized by multireference second-order perturbation theory [6] with appropriate orbitals included in the active space. The C—N and N—H bond fissions involve doublet and quartet PESs because of the parallel and antiparallel alignment of electron spins in the NH and CH_3N radicals. Since the energy of $NH(X\,^3\Sigma^-)$ is 42.73 kcal/mol lower than that of $NH(a\,^1\Delta)$, the reaction path leading to the $CH_3 + NH(X\,^3\Sigma^-)$ products is energetically favorable. This is also true in the case for the triplet, $^3CH_3N$ product formation. Therefore, the transition state structures in C—N and N—H bond fission reactions were determined for the triplet products formation. Specifically, for the $CH_3 + NH(X\,^3\Sigma^-)$ dissociation channel, the active space includes the bonding orbital between the p orbital of the N atom and the p orbital of the C atom, as well as a perpendicular p orbital for the radical on the NH fragment. Similarly, for the $^3CH_3N + H$ dissociation channel, the active space includes the bonding orbital between the p orbital of the N atom and the s orbital of the H atom, as well as a perpendicular p orbital for the radical on the CH_3N fragment. Such orbital configurations were included

in the active space of the transition state to acquire a parallel alignment of electron spins on the corresponding N atom for the formation of the triplet NH and $^3CH_3N$ products.

For the abstraction of amine hydrogen atoms by H atom, the multi-reference character of the wave functions was also found to be quite significant, as reflected by their T1 diagnostics [6] of 0.03 from QCISD(T)/cc-pVQZ calculations. The CASPT2 method with aug-cc-pVDZ and aug-cc-pVTZ basis sets was applied to optimize the geometries of reactants and transition states, and to calculate the ro-vibrational frequencies. In the CASPT2 geometry optimizations, the active space (4e,3o) was chosen for CH_3NHNH_2, consisting of the σ, $\sigma*$ orbital pair of the N—N bond and the s orbital of the amine N atom. The active space (3e,3o) consisting of the H atom orbital and the σ, $\sigma*$ orbital pair of the H atom being abstracted was chosen for the transition states for the abstraction of amine H atoms. For abstraction of the methyl H atom, the orbitals of the N—N and C—N bonds become delocalized. Consequently, a larger active space (7e,5o) consisting of the H atom orbital, the σ, $\sigma*$ orbital pair of the methyl H atom being abstracted, and the two hybrid orbitals between the methyl and the NH groups was chosen for the transition state for the abstraction of methyl hydrogen.

Higher-level single-point energies were determined from the spin unrestricted or restricted quadratic-configuration-interaction QCISD(T) calculations for open-shell and closed-shell species. The cc-pVTZ and cc-pVQZ basis sets were adopted in the QCISD(T) calculations and the energies were extrapolated to the complete basis set (CBS) limit, cc-pV∞Z, by the asymptotic form [7][8]. Electronic structure calculations were performed using the MOLPRO [9] and Gaussian09 [10] program packages.

3. Kinetics of CH₃NH Radical Decomposition

The thermal decomposition of the CH_3NH radicals was found to occur by the following reaction pathways:

$$CH_3NH \rightarrow TS1 \rightarrow CH_3 + NH \qquad (R1)$$

$$\rightarrow TS2 \rightarrow CH_2\text{=}NH + H \qquad\qquad (R2)$$

$$\rightarrow TS3 \rightarrow CH_2NH_2 \qquad\qquad (R3)$$

$$CH_2NH_2 \rightarrow TS4 \rightarrow CH_2\text{=}NH + H \qquad\qquad (R4)$$

$$CH_3NH \rightarrow TS5 \rightarrow CH_3N + H \qquad\qquad (R5)$$

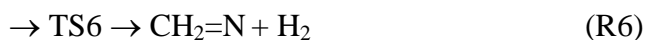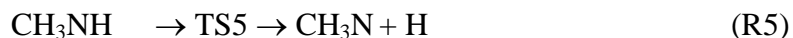$$\rightarrow TS6 \rightarrow CH_2\text{=}N + H_2 \qquad\qquad (R6)$$

Figure 1 shows the stationary points of the potential energy surfaces of the CH_3NH radical decomposition characterized at the UQCISD(T)//cc-pV∞Z level with CASPT2/cc-pVTZ and B3LYP/6-311++G(d,p) geometries. For the C—N bond fission (R1), a saddle point with a doublet state (TS1) was found to have an energy of 79.51 kcal/mol higher than that of the CH_3NH radical, and it is 2.98 kcal/mol higher than that of the $CH_3 + NH(X^3\Sigma^-)$ channel. The β scission of the methyl H atom from the CH_3NH radical was found to have an energy barrier of 33.08 kcal/mol, forming amino-methylene ($CH_2\text{=}NH$) (R2). Isomerization of the CH_3NH radical produces the CH_2NH_2 radical with an energy barrier of 36.39 kcal mol^{-1} (R3). The CH_2NH_2 radical formed also undergoes β scission of the amine H atom with an energy barrier of 39.37 kcal/mol, forming $CH_2\text{=}NH$ (R4). The N—H bond fission reaction in the CH_3NH radical that leads to the triplet $^3CH_3N$ radical and H atom is endothermic by 83.86 kcal mol^{-1} (R5). The doublet transition state (TS5) was found to have an energy of 0.54 kcal/mol lower than its products. A direct H_2 elimination from the CH_3NH radical is endothermic by 13.24 kcal mol^{-1} (R6), but its energy barrier is quite high, 99.62 kcal mol^{-1}, and is not kinetically relevant.

In the decomposition of CH_3NH radicals, micro-canonical rate coefficients as functions of total rotational-vibrational energy (E) and total angular momentum (J) were calculated using Rice–Ramsperger–Kassel–Marcus (RRKM) theory and multi-well master equation analysis [11][12][13] which were implemented in the VARIFLEX code [14]. Tunneling corrections were included for all transition states based on asymmetric Eckart potentials [15]. Pressure-dependent kinetics analysis was

performed by solving the time-dependent, multiple-well master equation. The collisional energy transfer probability in the master equation analysis was approximated by a single-exponential-down model, employing the temperature dependent form, $\Delta E_{down} = 200(T/300)^{0.85}$ cm^{-1}, for the average downward energy transfer [16]. The Lennard-Jones parameters for the collision rates were estimated to be $\sigma = 3.8$ Å and $\varepsilon = 253$ cm^{-1} for the CH$_3$NH radical, and $\sigma = 3.70$ Å and $\varepsilon = 66.1$ cm^{-1} for nitrogen [17].

We chose CH$_3$ + NH($X\ ^3\Sigma^-$) $\rightarrow$ CH$_3$NH (R-1) as an entrance channel to determine the phenomenological rate coefficients. At a pressure of 1 atm, the rate coefficients for three dominant decomposition channels (R2, R3, and R4) were obtained and fitted as the following expressions in the temperature range of 600 to 2500K.

$$k_2 = 2.69 \times 10^{27}\ T^{-4.767}\ \exp(-18598.9/T)\ \text{s}^{-1}$$

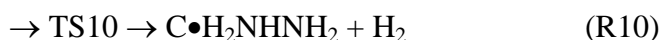$$k_3 = 1.02 \times 10^{30}\ T^{-6.038}\ \exp(-18823.9/T)\ \text{s}^{-1}$$

$$k_4 = 1.85 \times 10^{31}\ T^{-5.755}\ \exp(-22570.3/T)\ \text{s}^{-1}$$

It is noted that due to the uncertainties in the parameters for the average energy transfer model, the above pressure dependent rate coefficients need to be further quantified/validated by future experimental measurements. Nevertheless, these rate coefficients should be useful for kinetics analysis for the CH$_3$NH radical decomposition. Figure 2 shows the rate coefficients k_2, k_3, and k_4 at 1 atm along with the corresponding high-pressure limit rate coefficients in the range of 600 - 2500K. It is seen that the direct dissociation rate (k_2) to CH$_2$=NH + H is dominant at all temperatures. The dissociation rate (k_4) to CH$_2$=NH + H, is comparable to k_2 only when the temperature is above ~1800K. The isomerization rate coefficient (k_3) to CH$_2$NH$_2$ is about one order of magnitude smaller than k_2. This is ascribed to the tight three-center transition state (TS3) with an imaginary frequency of 1991.6 cm^{-1}, while the β scission of the methyl H atom occurs via a looser transition state (TS2) with an imaginary frequency of 555.4 cm^{-1}. Furthermore, strong pressure dependence in the dissociation rates is observed, and β scission of the

methyl H atom to form $CH_2=NH$ dominates at all pressures. Between 1 atm and the high pressure limit, the rate coefficient k_2 was found to be in the range from 1.6×10^6 to 8.7×10^7 s^{-1}, and is fast enough to produce H atoms that can subsequently abstract H atoms from unburned fuel molecules to trigger ignition. In the following section, the kinetics of H-abstraction from CH_3NHNH_2 by H atoms is analyzed.

4. Kinetics of H-Abstraction from CH_3NHNH_2 by H atom

For the direct abstraction of different H atoms from CH_3NHNH_2 by H atoms, four distinct radicals are possible, as shown in Figure 3.

$$CH_3NHNH_2 + H \quad \rightarrow TS7 \rightarrow CH_3N\bullet NH_2 + H_2 \qquad\qquad (R7)$$
$$\rightarrow TS8 \rightarrow \ trans\text{-}CH_3NHN\bullet H + H_2 \qquad\qquad (R8)$$
$$\rightarrow TS9 \rightarrow cis\text{-}CH_3NHN\bullet H + H_2 \qquad\qquad (R9)$$
$$\rightarrow TS10 \rightarrow C\bullet H_2NHNH_2 + H_2 \qquad\qquad (R10)$$

For the $CH_3NHN\bullet H$ radical, it is noted that the geometry with the terminal amine H atom trans to the methyl group is defined as the trans-$CH_3NHN\bullet H$ radical, and the geometry with the terminal amine H atom cis to the methyl group is defined as the cis-$CH_3NHN\bullet H$ radical. In these CASPT2 optimized transition state geometries, the cleaving N—H bond lengths are 1.137, 1.128, and 1.163 Å, and the forming H—H bond lengths are 1.071, 1.127, and 1.038 Å in TS7, TS8, and TS9, respectively. In TS10, the cleaving C—H bond length is 1.232 Å and the forming H—H bond length is 1.172 Å. In comparing the above cleaving and forming bond length data, it is seen that the formation of the trans-$CH_3NHN\bullet H$ radical via TS8 should be more facile because of the longer forming H—H bond length. This implies a low energy barrier in this channel and as such is the dominant reaction path.

With the optimized geometries in Figure 3, the rotational and vibrational frequencies of the four transition states were calculated at the same CASPT2/cc-pVTZ level. The T1 diagnostics, zero-point energies, and zero-point corrected UQCISD(T)/cc-pV∞Z energies relative to that of CH_3NHNH_2 + H channel are listed in Table 1. The four abstraction channels (R7 through R10) have energy barriers of 4.16, 2.95, 5.98, and 8.50 kcal mol^{-1}, respectively. The channels for the abstraction of amine H atoms are exothermic by 23 to 25 kcal mol^{-1}, while the channel for the abstraction of the methyl H atom is less exothermic (11.7 kcal mol^{-1}). The abstraction of a terminal amine H atom to form trans-$CH_3NHN\bullet H$ + H_2 (R8) has the lowest energy barrier of 2.95 kcal mol^{-1} among the four transition states, which is due to the longer forming H—H bond in TS8 as discussed above. It is expected to be the dominant channel among these abstraction reactions.

The rate coefficients of the above H-abstraction reactions were determined using (E, J) resolved micro-canonical transition state theory with the CASPT2/aug-cc-pVTZ optimized geometries and vibrational frequencies. Hindered rotor corrections for the C−N and N−N torsional modes were obtained from one-dimensional fits of the torsional potentials, employing Pitzer-Gwinn like approximations [18] and the $I^{(2,3)}$ moments of inertia that reproduced the coupled-harmonic-oscillator limit at low temperatures, and the free-rotor limit at high temperatures. Tunneling effects through the saddle points were modeled with asymmetric Eckart potentials. The imaginary frequencies of the four transition states used for the tunneling corrections are: 1895.4, 1674.7, 1969.9, and 2151.2 cm^{-1}, respectively, which were obtained from the CASPT2/cc-pVTZ calculations. The calculated rate coefficients for the abstraction of different H atoms in CH_3NHNH_2 by H atom are shown in Figure 4. The rate coefficient k_8 for the abstraction of the terminal amine H atom to form trans-$CH_3NHN\bullet H$ + H_2 dominates below 1500K. Furthermore, the rate coefficient k_8 is within the lower limit of the reported experimental rate coefficient at 298K [5], which implies that the channel (R8) is the predominant

abstraction channel. Due to the small energy barrier, tunneling effects on k_8 are expected to be significant at low temperatures. The tunneling factor for k_8 was found to be in the range of 6.20 - 1.71 for temperatures in the range of 298 - 600K, and decreases to 1.37 - 1.04 in the higher temperature range of 800 - 2500K. The abstraction of the central amine H atom (R7) becomes dominant above 1500K, whereas reactions (R9) and (R10) become important at temperatures above 1000K. It is seen that the reactions are governed by the abstraction of the amine hydrogen atoms at low temperatures, and the abstraction of the methyl H atoms becomes important at high temperatures. Furthermore, β-scission of NH_2 from the $C\bullet H_2NHNH_2$ radical is the fastest process among the decomposition channels of the four radicals [19]. Therefore all of the abstraction channels are important pathways in the CH_3NHNH_2 pyrolysis/oxidation. In units of cm^3 molecule^{-1} s^{-1}, the rate coefficients were fitted as follows:

$$k_7 = 9.63 \times 10^{-20} \, T^{2.596} \exp(-154.2/T)$$

$$k_8 = 2.04 \times 10^{-18} \, T^{2.154} \exp(104.1/T)$$

$$k_9 = 1.13 \times 10^{-20} \, T^{2.866} \exp(-416.3/T)$$

$$k_{10} = 2.41 \times 10^{-23} \, T^{3.650} \exp(-870.5/T)$$

Assuming the rate coefficients are additive, the total rate coefficient k_{total} was determined to be $2.55 \times 10^{-20} \, T^{2.896} \exp(227.6/T)$ cm^3 molecule^{-1} s^{-1}. At room temperature, the theoretical rate coefficient is 8.16×10^{-13} cm^3 molecule^{-1} s^{-1}, and as seen in Figure 4, it is in the upper bound of the experimental observation of $(7.60 \pm 1.14) \times 10^{-13}$ cm^3 molecule^{-1} s^{-1} [5]. The excellent agreement between theory and experiment for the total rate coefficient at room temperature gives us confidence in the accuracy of the theoretical rate coefficients at high temperatures. Based on these theoretical rate coefficients, the branching ratios as a function of temperatures are plotted in Figure 5. k_8 for forming the trans-$CH_3NHN\bullet H$ radical is shown to be the predominant rate coefficient among all of the abstraction channel

rate coefficients for temperatures below 1200K. This is consistent with our previous study on the related H atom abstraction from CH_3NHNH_2 by OH radicals [20].

Recently, a kinetics analysis on the reactions of CH_3NHNH_2 + H/D was performed by Wang et al. [21] based on quantum chemistry calculations at the MCG3-MPWPW91//MPW1K/6-311G(d,p) level, which yielded a value for the total rate coefficient of $1.47 \times 10^{-19} T^{2.74} exp(-239.1/T)$ cm^3 molecule^{-1} s^{-1} in the temperature range of 200 to 2000K. Their calculated total rate coefficient at 298K is 4.14×10^{-13} cm^3 molecule^{-1} s^{-1}, which is a factor of 2 lower than the experimental value [5]. The discrepancy in the total rate coefficient value between the study of Wang *et al*. [21] and this work is in the range 2 - 0 .7 in the temperature range of 300 - 2500K. In their analysis, Wang *et al.* considered the H-abstraction reactions of two CH_3NHNH_2 isomers with six distinguishable pathways for each isomer. The rate coefficient for each reaction channel was calculated by using canonical variational transition state theory with a small-curvature tunneling correction (CVT/SCT), and all of the rotational and vibrational frequencies were treated by the harmonic-oscillator approximation. The total rate coefficient was determined by summation of the individual rate coefficient contributions from each of the isomers using weighting factors in the Boltzmann distribution function. Furthermore, they concluded that the H atom abstraction from the central NH group is the dominant channel below 500K, which is contrary to our findings. We note here that the branching ratios will certainly affect the radical product distributions when modeling CH_3NHNH_2 pyrolysis and oxidation.

In this work, we have carried out high-level UQCISD(T)/cc-pV∞Z//CASPT2/aug-cc-pVTZ calculations to obtain accurate values for the molecular properties and energy values for the species involved in this system. The rate coefficient was computed by micro-canonical transition state theory with conservation of total rotational-vibrational energy (E) and total angular momentum (J), and the torsional anharmonicities were treated as internal rotations for the rotational conformers. Consequently,

our approach should provide a better perspective for the branching ratios as well as absolute values of the temperature dependent rate coefficients.

5. Concluding Remarks

The kinetics of the thermal decomposition of CH_3NH radicals was analyzed and pressure dependent rate coefficients of the dominant reaction pathways were determined by RRKM master equation analysis. β scission of methyl H atom to form the $CH_2=NH$ product was found to be the most dominant channel in the CH_3NH radical decomposition. Furthermore, the kinetics of H-abstraction from CH_3NHNH_2 by H atoms was analyzed using second-order multireference perturbation theory and unrestricted quadratic-configuration-interaction QCISD(T) calculations. The rate coefficient for each channel was calculated at the (*E, J*) resolved level using micro-canonical transition state theory, and the corresponding branching ratios for the product channels determined. The results reveal that the abstraction of the terminal amine H atom to form trans-$CH_3NHN•H$ radical is the most dominant channel among all the abstraction channels. The total theoretical rate coefficient computed is in excellent agreement with the available experimental data.

References

[1]   E. W. Schmidt, Hydrazine and its derivatives: preparation, properties, applications 2nd ed., John Wiley & Sons, Inc., New York, **2001**.

[2]   H. Sun, C. K. Law, *J. Phys. Chem. A* **2007**, *111*, 3748-3760.

[3]   P. Zhang, S. J. Klippenstein, H. Sun, C. K. Law, *Proc. Combust. Inst.* **2011**, *33*, 425-432.

[4]   S. Li, D. F. Davidson, R. K. Hanson, *Combust. Flame* **2014**, *161*, 16-22.

[5]   G. L. Vaghjiani, *J. Phys. Chem. A* **1997**, *101*, 4167-4171.

[6]   H.-J. Werner, P. J. Knowles, *J. Chem. Phys.* **1985**, *82*, 5053-5063.

[7]   J. M. L. Martin, *Chem. Phys. Lett.* **1996**, *259*, 669-678.

[8]   D. Feller, D. A. Dixon, *J. Chem. Phys.* **2001**, *115*,3484-3495.

[9]   Werner, H.-J.; Knowles, P. J.; Knizia, G.; Manby, F. R.; Schütz, M. and others, MOLPRO, version 2010.1, a package of *ab initio* programs, see http://www.molpro.net.

[10]   Frisch, M. J.; Trucks, G. W.; Schlegel, H. B.; Scuseria, G. E.; Robb, M. A.; Cheeseman, J. R.; Scalmani, G.; Barone, V.; Mennucci, B.; Petersson, G. A. et al. Gaussian 09, Revision A.1, Gaussian, Inc., Wallingford CT, 2009.

[11]   J. A. Miller, S. J. Klippenstein, *J. Phys. Chem. A* **2006**, *110*, 10528-10544.

[12]   A. Fernández-Ramos, J. A. Miller, S. J. Klippenstein, D. G. Truhlar, *Chemical Reviews* **2006**, *106*, 4518-4584.

[13]   J. A. Miller, S. J. Klippenstein, *J. Phys. Chem. A* **2003**, *107*, 2680-2692.

[14]   Klippenstein, S. J.; Wagner, A. F.; Dunbar, R. C.; Wardlaw, D. M.; Robertson, S. H.; Miller, J. A.; VARIFLEX: version 2.02m, 2010.

[15]   H. S. Johnston, J. Heicklen, *J. Phys. Chem.* **1962**, *66*, 532-533.

[16]   J. A. Miller, S. J. Klippenstein, *Phys. Chem. Chem. Phys.* **2004**, *6*, 1192-1202.

[17]   J. O. Hirschfelder, C. F. Curtiss, R. B. Bird, Molecular theory of gases and liquids, Wiley, New York, **1954**.

[18]   K. S. Pitzer, W. D. Gwinn, *J. Chem. Phys.* **1942**, *10*, 428-440.

[19]   H. Sun, P. Zhang, C. K. Law, *J. Phys. Chem. A* **2012**, *116*, 8419-8430.

[20]   H. Sun, P. Zhang, C. K. Law, *J. Phys. Chem. A* **2012**, *116*, 5045-5056.

[21]   L. Wang, Y. Zhao, J. Wen, J. Zhang, *Theor. Chem. Accounts* **2013**, *132*, 1321.

TABLE1. Molecular Properties for CH_3NHNH_2 + H Reaction

Transition state	T1 diagnostic [a]	ZPE [b]	ΔE [c]	ΔE [d]
TS7_$CH_3N \bullet NH_2$	0.029	49.76	4.16	4.27
TS8 _trans-$CH_3NHN \bullet H$	0.031	50.13	2.95	3.44
TS9_cis-CH3NHN•H	0.028	49.79	5.98	5.91
TS10_C•H_2NHNH_2	0.018	50.08	8.50	8.11

[a] T1 diagnostics calculated at the QCISD(T)/cc-pVQZ level. [b] Zero-point energy calculated at the CASPT2/aug-cc-pVTZ level, units in kcal mol^{-1}. [c] Zero-point corrected energy relative to the reactants CH_3NHNH_2 + H calculated at the QCISD(T)/cc-pV∞Z//CASPT2/aug-cc-pVDZ level, units in kcal mol^{-1}. [d] Zero-point corrected energy relative to the reactants CH_3NHNH_2 + H calculated at the MCG3-MPWPW91 //MPW1K/6-311G(d,p) level by Wang et al. [21], units in kcal mol^{-1}.
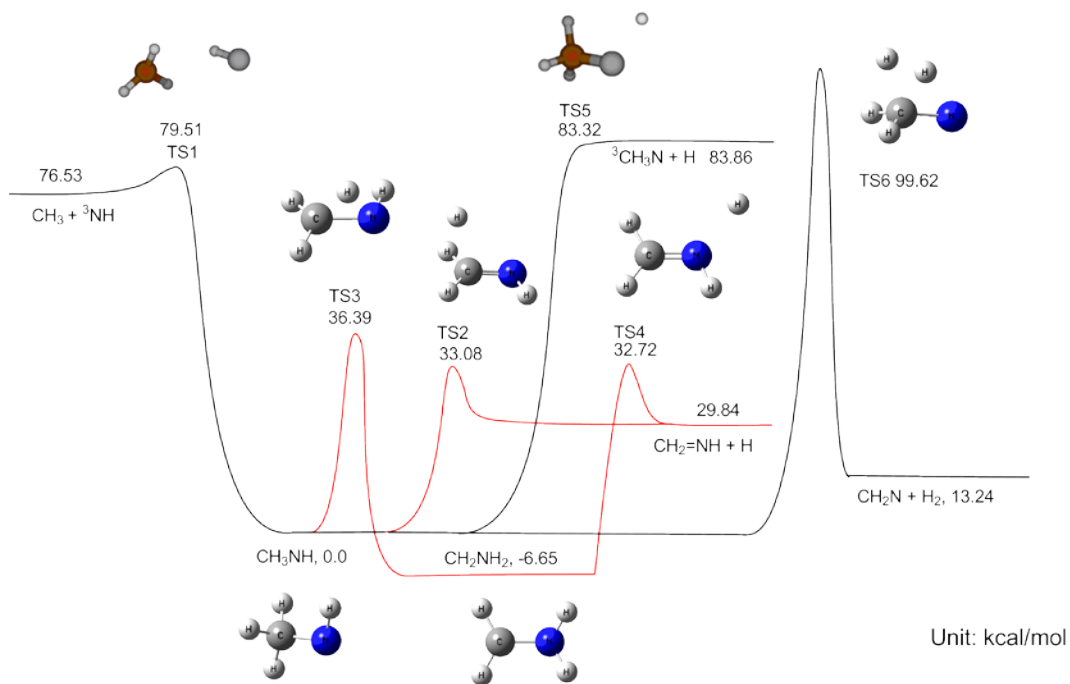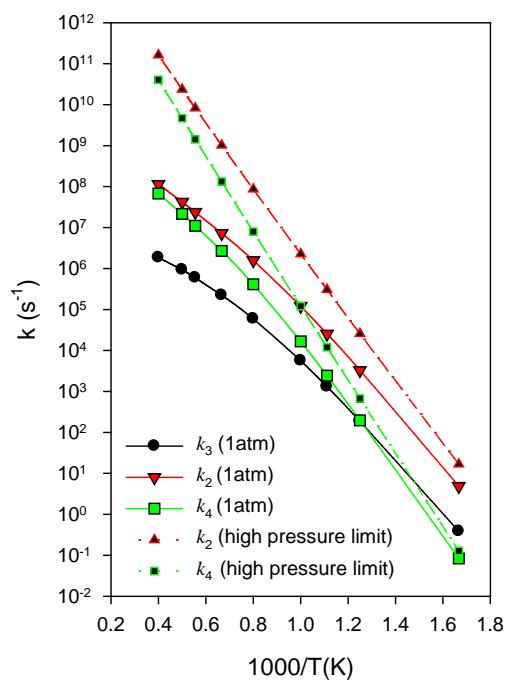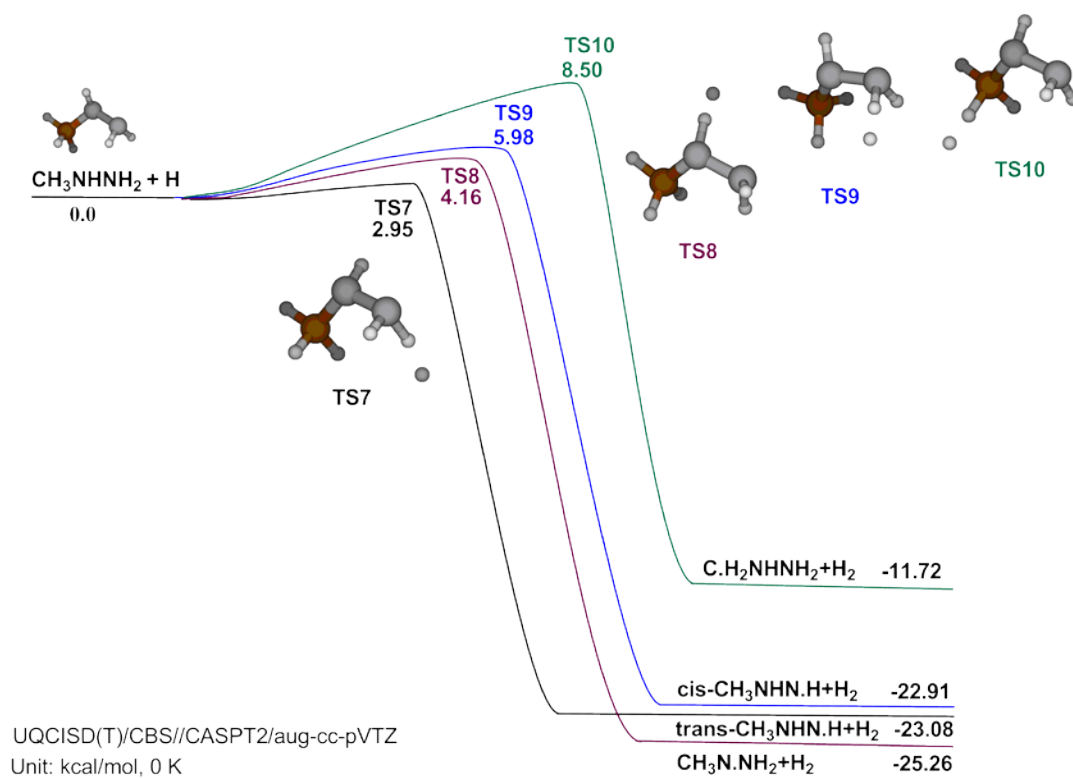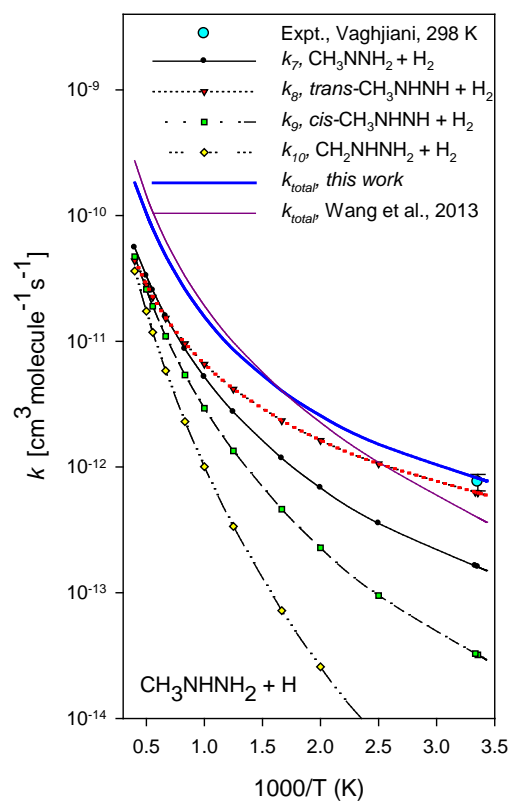
Figure 1

Figure 2

Figure 3

Figure 4

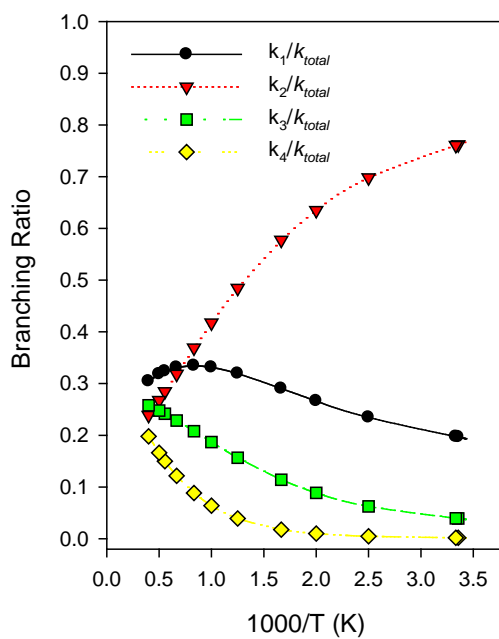# Figure 5

Figure Captions

Figure 1. Potential energy surfaces for $CH_3N•H$ radical decomposition.

Figure 2. Rate coefficients of CH_3NH radical dissociation in the temperature range 600 -

2500K.

Figure 3. Potential energy surfaces for $CH_3NHH_2 + H$ reaction calculated at the UQCISD(T)/cc-pV∞Z//CASPT2/aug-cc-pVTZ level.

Figure 4. Theoretical abstraction rate coefficients for $CH_3NHH_2 + H$ reaction, with comparison of experimental data.

Figure 5. Theoretical abstraction branching ratios for $CH_3NHH_2 + H$ reaction as a function of temperature.